Optimal Scheduling of Integrated Energy Systems for High-speed Railway Stations Considering Integrated Demand Response under the Carbon Market

Lei Hou, Hui jie Lin, Xin Yang, Tian kuo Yang, Feng Qu and Dan Shao

***Abstract*—An integrated energy system (IES) can significantly enhance utilization efficiency and boost renewable energy consumption while also catering to various energy needs within the system. It is one of the essential models of future energy system development. With a focus on improving carbon market subjects and carbon transaction mechanisms, this paper proposes integrated energy optimization scheduling in high-speed railway stations considering demand response under the participation of the carbon market, considering both low-carbon and economic needs. In the context of participation in the carbon and energy markets, an integrated energy system in the high-speed railway station is constructed, comprising photovoltaic power generation, stored energy device, CCHP and gas boiler. Based on the simulations of each energy device, the demand response compensation price and carbon transaction revenue are taken into account, and the target is to economize the operating budget and optimize the arrangement for IES in a high-speed railway station under the carbon transaction market. Through simulation, the optimization performance of the proposed model is analyzed under the conditions of demand response and no carbon cap-and-trade market. The findings demonstrate that the best scheduling strategy for integrated energy at high-speed rail stations taking into account integrated demand response under the carbon market can successfully reduce carbon emissions from station operation while flattening the peak-to-valley load difference on the grid side, opening up ideas for the proposal of energy saving and emissions reduction.**

***Index Terms*—high-speed railway station, carbon transaction, integrated energy, optimal scheduling**

Manuscript received September 6, 2022; revised March 14, 2023.

This work is supported by Science and Technology project of State Grid Corporation (Multi-energy collaborative optimization and intelligent management and control technology of high proportion clean energy high-speed railway stations, NO. 5100-202113396A-0-0-00)

Lei Hou is a senior associate engineer of State Grid Xiong'an New Area Electric Power Supply Company, Baoding 071600, China, (e-mail: 705608320@qq.com).

Hui jie Lin is an engineer of NARI-TECH Nanjing Control Systems Co., Ltd., Nanjing 211106, China, (Corresponding author, e-mail: lhj19971224@126.com).

Xin Yang is an engineer of State Grid Xiong'an New Area Electric Power Supply Company, Baoding 071600, China, (e-mail: 516898598@qq.com).

Tian kuo Yang is an engineer of State Grid Xiong'an New Area Electric Power Supply Company, Baoding 071600, China, (e-mail: ytk1991@163.com).

Feng Qu is an engineer of State Grid Xiong'an New Area Electric Power Supply Company, Baoding 071600, China, (e-mail: 81741684@qq.com).

Dan Shao is a mid-level engineer of State Grid Xiong'an New Area Electric Power Supply Company, Baoding 071600, China, (e-mail: shaodan3770@126.com).

I. Introduction

In this context, the integrated energy system [1](IES) combines coal, oil, gas, electricity, heat and other energy sources in a certain district and realizes coordinated planning, optimal performance, synergistic regulation, cooperative response and complementarity between various energy components. Currently, demonstration projects for building-level IESs [2] are already underway, with a series of successive results [3]-[5]. In [3], an optimal dispatch strategy for building IESs that takes human behavior into account is proposed. Both the impacts of warmth comfort and intention to participate in orderly EV charging are analyzed. The literature [4] applies an economical assessment model of intelligent communities under arbitrary conditions, such as electricity prices and photovoltaic power generation fees. The study in Paper [5] evaluates a new system for sharing green electricity from PV using V2G technology and develops a graphical partitioned spatial clustering algorithm based on meta-heuristics to find the best spatial clusters that minimize the differences between power surplus and stock potential.

As a large transportation building that is a hub for the comprehensive passenger transport of the high-speed railway station [6](HRS), the internal energy supply system in an HRS couples all sorts of energy, such as cooling, thermal and electricity [7], and the energy-using system includes charging piles [8]-[10], which has become one of the representative scenarios for applying IESs. Through integrated energy demand response (DR) scheduling [11], popular topics in current research include breaking down the barriers of various energy subsystems in HRSs, achieving the advantageous complementary and ladder utilization of multiple types of energy, meeting the multiple load demands on the user side of the station, improving the effectiveness of total energy utilization, and enhancing the economy and reliability of the energy supply networks of stations.

Many scholars have carried out studies on the operation in HRSs, where the external energy market is a decisive factor in the operation of HRSs. The literature [12], [13] mainly considers the external energy market as the main influence mechanism of an IES. The literature [12] provides a technical and financial comparison of several arrangements with power electronic converters incorporating photovoltaic resources in HRS power systems. The analysis suggests that as PV resources are gradually integrated into the railway

system, configurations powered by power converters may become more favorable than the more classic solutions of powering overhead lines via transformers. In the literature [13], through the analysis of the energy usage of HRSs in southern China, we can explicitly identify the energy usage of each type of power and recommend appropriate strategies to preserve the energy. The import of electricity from the grid can be kept at a relatively low level due to the contribution of PV and ESS. By developing better energy management strategies, it is possible to pursue further energy reduction and eco-friendly goals. Furthermore, [14]-[17] considers the volatility of external energy markets. A nonlinear controller for a low-level distributed DC microgrid installed in an intelligent train station is presented in [14], and it could recover the braking energy of the train. In addition, the paper proposes a stratified control structure and system control strategy and analyses its stability. The results demonstrate that the method is highly appropriate for different renewable resources, loads and storage equipment selection and capacity planning. In [15], the prospects, special features and possibilities of solar power systems for roofs in railway stations will be discussed to boost the energy productivity of railways. The literature [16] presents an optimized study of mixed railway power substation energy administration and develops a fuzzy logic regulatory scheme to harmonize renewable energy sources and storage units in railway substations. The literature [17] proposes a scalable, adaptive, independent, and smart distributed generator. It can be connected to the conduit as a solution to the problems related to transportation railroads because of the distributed control of the DC bus of a multiagent system.

With the promotion of the national carbon emission reduction target and energy structure optimization and adjustment target, the carbon transaction market structure is becoming increasingly better, and importing carbon transactions to balance the economics and environmental protection of an IES is necessary. In the literature [18], due to the use of renewable energy and integrating ESSs into railway power systems, the request for grid power declines, and a lower carbon fee is charged. Although existing studies have actively explored the optimal operation of IESs in HRSs, they have not yet considered the participation of HRSs in the carbon market. Moreover, optimizing IESs in HRSs to achieve both economic and environmental reductions under consideration of the carbon market deserves our in-depth study.

To address the above issues, a DR optimization scheduling strategy that participates in the carbon transaction[19] mechanism and takes into account the comfort level[20] of the user side in an HRS is provided in this paper. First, according to the flexible features and responsiveness of electric, thermal and cooling loads, the output curves of electric, thermal and cooling loads are dynamically adjusted to optimize the energy utilization efficiency in an HRS. Finally, the proposed model is solved using the CPLEX solver. The analysis of the simulation shows that the suggested approach can validly maximize the revenue of the HRS, fully utilize the DR potential of the consolidated energy in the station, and achieve a lower operation expense of the station.

II. Integrated Energy System Operation Architecture for High-Speed Railway Stations

A. Integrated Energy Physical Architecture for High-Speed Railway Stations

Due to their functional positioning and urban status, the internal space structure and load properties in the HRSs are different from those of ordinary buildings. In the background of the national promotion of a green and low-carbon economy, the implementation of a combined cooling heating and power (CCHP) into an HRS can not only provide station users with multiple load requirements for heating and cooling but also increase the reliability of the power delivery in the station and maintain the secure operation of the HRS. The main electricity supply devices of the joint power system in the HRS are photovoltaic power generation, gas turbines, storage batteries, and V2B dispatching, which also interact with the main network in the grid-connected operation mode; auxiliary heating subequipment includes gas boilers and waste heat boilers; and cooling subequipment mainly includes absorption chillers and electric chillers. In summary, an illustration of the IES in the HRS is shown in Fig. 1.

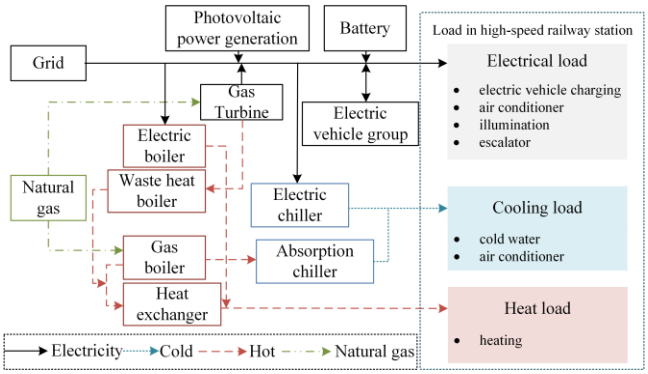

Fig. 1. IES Architecture in HRSs.

In such a situation, the load-side cooling, thermal and electrical load balance equations are as described below.

(1) Electrical power balance constraint:

$$\sum_{i=1}^{N_{DG}} P_{Gi,t} + P_{g,t} + P_{EV\_rat} + P_{ch,t} - P_{dis,t} = P_{L,t} \tag{1}$$

where $P_{Gi,t}$ refers to the *ith* distributed power source during time *t*; $P_{g,t}$ refers to the exchanged power between HRS and the grid during time *t*; an over 0 value indicates that the HRS sells electricity to the grid, while a less than 0 value means that the HRS purchases electricity from the grid; P_{EV_rat} denotes the electric vehicle charging power rating, kW; $P_{ch,t}$ is denoted as the battery charging power during time *t*; $P_{dis,t}$ refers to the battery discharging power ; and $P_{L,t}$ refers to the electrical load power.

(2) Thermal power balance constraint:

$$\sum_{i=1}^{N_{MT}} H_{i,t} + H_{B,t} + H_{EB,t} = H_{D,t} \tag{2}$$

where N_{MT} refers to the number of gas turbines; $H_{i,t}$ refers to the gas turbine operating thermal power; $H_{B,t}$ is the make-up boiler thermal power; $H_{EB,t}$ is the electric boiler thermal power; and $H_{D,t}$ is denoted as the thermal load power.

(3) Cold power balance constraint:

$$Q_{AC,t} + Q_{EC,t} = Q_{C,t} \tag{3}$$

where $Q_{AC,t}$ refers to the absorption refrigerant's cooling power during time t; $Q_{EC,t}$ refers to the electric chiller's cooling power; and $Q_{C,t}$ refers to the system cooling load power during time t.

B. Integrated Energy Operation Architecture for High-Speed Railway Stations

Carbon transactions are considered to be an effective means to enhance the environmental benefits of the system while taking into account the economics. In terms of new energy generation, HRSs have a large roof area and a strong load, which meets the basic conditions for the establishment of photovoltaic power generation. In terms of energy use, HRSs are characterized by high loads. Therefore, HRSs are endowed with very large space for carbon market development, and the economic returns are very considerable. The operational structure is shown below.

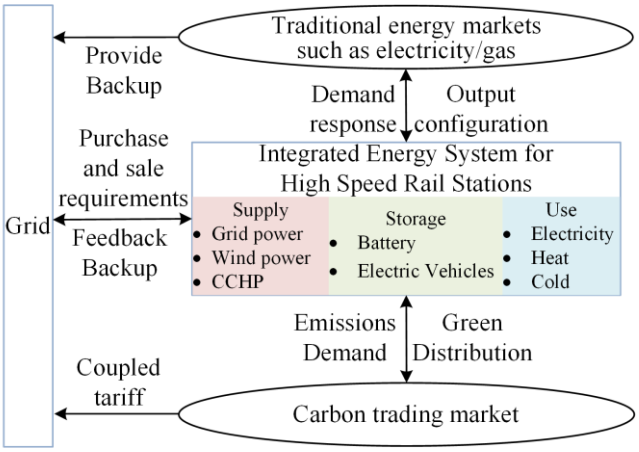

Fig. 2. Operational Architecture of the IES in the HRS.

In the traditional energy market, the IES in the HRS takes into account the peak and valley characteristics of electricity consumption and, according to the time-sharing tariff policy, improves the ability of the grid to sharpen peaks and fill valleys through interactions with the power grid and obtains economic benefits from it. This will enable the station to operate economically and environmentally under the constraints of carbon quotas.

The carbon transaction model of HRSs in the carbon market, which considers into account the dynamic price of carbon, can be established based on the nonreimbursable carbon quotas allocated to the station, and the amount of carbon emission rights traded can be characterized as follows:

$$E_{\text{PIES}} = E_{\text{PIES,r}} - E_{\text{PIES},a} \tag{4}$$

where E_{PIES} is denoted as the amount of carbon emission rights traded for the IES in an HRS; $E_{\text{PIES,r}}$ is the total carbon allowance of the IES of an HRS, which is a known fixed value; and $E_{\text{PIES},a}$ is the real carbon footprint of an IES in an HRS. To minimize carbon emissions, a stepped carbon transaction cost model is employed, which is computed as follows:

$$f_c = \begin{cases} \lambda E_{\text{PIES}} & E_{\text{PIES}} \leqslant l \\ \lambda(1+\sigma)\left(E_{\text{PIES}} - l\right) + \lambda l & l \leqslant E_{\text{PIES}} \leqslant 2l \\ \lambda(1+2\sigma)\left(E_{\text{PIES}} - 2l\right) + \lambda(2+\sigma)l & 2l \leqslant E_{\text{PIES}} \leqslant 3l \\ \lambda(1+3\sigma)\left(E_{\text{PIES}} - 3l\right) + \lambda(3+3\sigma)l & 3l \leqslant E_{\text{PIES}} \leqslant 4l \\ \lambda(1+4\sigma)\left(E_{\text{PIES}} - 4l\right) + \lambda(4+6\sigma)l & 4l \leqslant E_{\text{PIES}} \end{cases} \tag{5}$$

where f_c refers to the stepped carbon transaction cost; Base transaction price is indicated by λ, while the carbon emissions interval is indicated by l; and σ refers to the carbon price growth rate. It is notable that when $E_{\text{PIES,r}} < E_{\text{PIES},a}$, i.e., $E_{\text{PIES}} < 0$, the practical carbon emissions of the IES in the HRS are lower than allowances, money can be made by trading carbon allowances at the original carbon transaction price.

III. Integrated Energy System Physical Model for High-Speed Railway Stations

A. Modeling of Power Generation Systems

In the HRS, the power generation equipment of IES primarily consists of photovoltaic generators and gas turbines, whose models have been studied in a large amount of literature and will not be repeated here in this paper. The specific formulae can be found in the literature [1-4].

B. Modeling of an Energy Storage System

Energy storage systems (ESSs) are an indispensable part of the IES in HRSs. Among the many energy storage devices, the battery is inexpensive, the energy storage technology is relatively developed, and it is a common energy storage appliance in the microgrid. Therefore, in the IES of the HRS, the main consideration of ESSs is to use the battery.

Regarding the battery charging and discharging process, the state of charge (SOC) of the battery at time t is related to the state of charge at time t-1, battery charging and discharging between time t-1 and t and the hourly battery decay amount.

When the battery is charging, the SOC can be characterized as:

$$S_{OC,t} = S_{OC,t-1}(1-\sigma) + \eta_c \frac{P_{ch,t}\Delta t}{Q_{bat}} \tag{6}$$

When the battery is discharging, the SOC can be characterized as:

$$S_{OC,t} = S_{OC,t-1}(1-\sigma) - \frac{P_{\text{dis},t}\Delta t}{Q_{bat}\eta_d} \tag{7}$$

where $S_{OC,t}$ is the SOC of the battery; σ is denoted as the self-discharge rate of the battery; η_c and η_d are denoted as the charging efficiency and discharging efficiency of the battery, respectively; $P_{ch,t}$ refers to the charging power of the battery; $P_{\text{dis},t}$ refers to the discharging power of the battery; Q_{bat} refers to the capacity of the battery; Δt is the time span.

C. Modeling of the Charging System

Considering the charging and discharging process model of an individual EV [21] of V2B, the charging process is

divided into several equal time periods, where the control state of the charging post can be adjusted at each time point. Moreover, both the power and state of the EV remain the same during each control period. Then, the EV model that accepts the scheduling can be expressed as:

$$\begin{aligned} 0 \leqslant P_{i,t}^{\mathrm{evc}} \leqslant P_{\max}^{\mathrm{evc}} x_{i,t}^{\mathrm{ev}} \\ 0 \leqslant P_{i,t}^{\mathrm{evd}} \leqslant P_{\max}^{\mathrm{evd}} \left(1 - x_{i,t}^{\mathrm{ev}}\right) \\ P_{i,t}^{\mathrm{evc}} = 0, P_{i,t}^{\mathrm{evd}} = 0 \quad t < t_i^{\mathrm{start}} \text{or } t > t_i^{\mathrm{end}} \end{aligned} \tag{8}$$

where $P_{i,t}^{\mathrm{evc}}$ and $P_{i,t}^{\mathrm{evd}}$ are denoted as the *ith* EV charging and discharging power; $P_{\max}^{\mathrm{evc}}$ and $P_{\max}^{\mathrm{evd}}$ refer to the rated power of the V2B smart charger, respectively; $x_{i,t}^{\mathrm{ev}}$ is the *ith* EV charging state variable during time *t*, which takes the value of 1 when charging and 0 when discharging; and t_i^{start} and t_i^{end} are the time when the *ith* EV arrives and leaves the charger, respectively.

To prolong the life-span of the power battery, the charge state constraint of the EV in V2B mode is set as shown in (9).

$$S_{\min}^{\mathrm{ev}} \leqslant S_{i,t}^{\mathrm{ev}} \leqslant S_{\max}^{\mathrm{ev}} \tag{9}$$

$$S_{i,t}^{\mathrm{ev}} = S_{i,t-1}^{\mathrm{ev}} + \frac{\Delta t}{Q_{\mathrm{ev}}}\left(P_{i,t}^{\mathrm{evc}} \eta^{\mathrm{evc}} - \frac{P_{i,t}^{\mathrm{evd}}}{\eta^{\mathrm{evd}}}\right) \tag{10}$$

where $S_{i,t}^{\mathrm{ev}}$ refers to the SOC of the *ith* EV; $S_{\min}^{\mathrm{ev}}$ and $S_{\max}^{\mathrm{ev}}$ are denoted as the minimum and maximum allowable EV charge states, respectively; Q_{ev} is the capacity of the EV power battery; and η^{evc} and η^{evd} are denoted as the charging and discharging efficiencies. The EV must be charged to the desired value when it leaves the charging post in order to assure the charging effect for the user. The number of EVs charging at the charging piles at the HRS in one day is set to be n^{ev}. The total charging power and total discharging power of the group of smart charging piles in time period t are $P_{i,t}^{\mathrm{evc}}$ and $P_{i,t}^{\mathrm{evd}}$, respectively.

$$P_t^{\mathrm{evc}} = \sum_{i=1}^{n^{\mathrm{ev}}} P_{i,t}^{\mathrm{evc}} \tag{11}$$

$$P_t^{\mathrm{evd}} = \sum_{i=1}^{n^{\mathrm{ev}}} P_{i,t}^{\mathrm{evd}} \tag{12}$$

D. Modeling of the Electrical System

As electricity consumption in HRSs is mainly considered in terms of utility and economy, user comfort is also gradually being taken into account. Controllable dynamic load power and working hours have adjustable characteristics, which have a very strong relationship with user comfort. The normal human body is not sensitive to temperature changes in the external environment within a certain range, and even if the supply of hot and cold power is adjusted to the temperature demand, the effect on human comfort is not obvious. According to the predicted mean vote (PMV), the perception of the human body regarding the ambient temperature can be divided into five stages, and the relationship between the two is shown in Table I.

TABLE I
PMV EVALUATION RULES

Comfortable level	HOT	Warm	Comfortable	Cool	Cold
PMV	-3	-1	0	+1	+3

At different ambient temperatures, the PMV will vary accordingly, and the functional relationship χ_{PMV} can be expressed as:

$$\chi_{\mathrm{PMV}} = \begin{cases} 0.39\left(T - T_0\right), T \geqslant T_0 \\ 0.41\left(T_0 - T\right), T \leqslant T_0 \end{cases} \tag{13}$$

where T indicates the room temperature; T_0 is the optimum ambient temperature for the human body, and relevant studies have shown that human comfort is highest when T_0 is 26°C. According to the regulations, comfort is best when χ_{PMV} is in the range of -0.5 to 0.5, so the above equation gives a range of values for T between 24.7°C and 27.2°C. Because there is a certain threshold of indoor temperature, the cooling and thermal load curve can be divided into several cooling and thermal load adjustment intervals within the temperature T so that it is transformed into a flexible load and the supply of cooling and thermal energy is regulated within the temperature threshold. Below is a representation of the link between interior temperature, comfort, and power supply as a function of temperature:

$$\frac{\mathrm{d}T}{\mathrm{d}t}\left(C_{\mathrm{a}} M_{\mathrm{a}} + C_{\mathrm{b}} M_{\mathrm{b}}\right) = Q_t^{\mathrm{L}} + \sum_{i=c/\mathrm{h}} Q_t^i \tag{14}$$

$$Q_t^{\mathrm{L}} = Q_t^{\mathrm{out}} + Q_t^{\mathrm{air}} + Q_t^{\mathrm{in}} \tag{15}$$

$$\begin{cases} Q_t^{\mathrm{out}} = \eta S_{\mathrm{h}}\left(T - T_{\mathrm{out}}\right) \\ Q_t^{\mathrm{air}} = C_{\mathrm{a}} \rho_{\mathrm{a}} V_{\mathrm{a}}\left(T - T_{\mathrm{out}}\right) \\ Q_t^{\mathrm{in}} = S\left(Q_{\mathrm{e}} + Q_{\mathrm{B}}\right) \end{cases} \tag{16}$$

where C_{a} and C_{b} are the specific thermal capacities of the air and the building wall of the HRS, respectively; M_{a} and M_{b} are the masses of the air and the building wall, respectively; Q_t^{L} is the overall load inside the HRS; Q_t^c and Q_t^h are the cooling and thermal power supplied inside the HRS during time *t*, respectively; and Q_t^{out}, Q_t^{air}, and Q_t^{in} are the thermal transfer from the external environment, the thermal transfer from the external air and the internal thermal exchange inside the building during time *t*, respectively. η indicates the heating transfer coefficient of the building wall; S_{h} is the heat conduction zone; ρ_{a} is the air density inside the building; V_{a} is the total amount of air exchange; T_{out} is the ambient temperature outside the building; S is the total area of the building; and Q_{e} and Q_{B} are the thermal energy provided by the electric heating equipment inside the building and the human body, respectively. The correspondence between the ambient temperature and human comfort can be used to derive the most comfortable temperature range for the human body at a certain time, and the adjustment range for the thermal and cooling power to be supplied to the building can be calculated, thus obtaining a thermal and cooling power scheduling plan that meets human comfort.

IV. MODELING THE OPTIMIZATION OF INTEGRATED ENERGY SYSTEMS IN HIGH-SPEED RAILWAY STATIONS CONSIDERING CARBON TRANSACTIONS

A. Objective Function

The target of the joint multienergy optimal dispatching of

the HRS is to satisfy the demand of the system for electricity, thermal and cooling and to minimize the fluctuation of the load in the station and the comprehensive operating cost of the station. The multienergy dispatching model developed in this paper is divided into two components.

(1) Minimal load fluctuations within the system:

$$F_1 = \min \sum_{t=1}^{N_T} (P_{load} + \sum_{i=1}^{N_{DG}} P_{Gi,t} - P_{EV,t}) \tag{17}$$

(2) The minimal overall operating costs of the system consider the O&M costs of the system equipment, the expense of natural gas, the expense of interaction with the parent grid and the expense of system participation in carbon transactions, based on the IES traditional day-ahead optimal dispatch method:

$$F_2 = \min(f_{ope} + f_{gas} + f_{grid} + f_C) \tag{18}$$

$$f_{ope} = \sum_{t=1}^{N_T} \sum_{i=1}^{N_{DG}} \left[C_f (P_{Gi,t}) + C_{OM} (P_{Gi,t}) \right] \tag{19}$$

$$f_{gas} = \sum_{t=1}^{N_T} \sum_{j=1}^{N_B} c_{gas} H_{Bj,t} / \eta_{Bj} + \sum_{t=1}^{N_T} \sum_{j=1}^{N_X} c_{gas} S_{xj,t} / \eta_{xj} \tag{20}$$

$$f_{grid} = \sum_{t=1}^{N_T} \left[C_{pp} (P_{g,t}) - I_{sp} (P_{g,t}) \right] \tag{21}$$

$$P_{g,t} = P_{load,t} - P_{G,t} + P_{EV,t} \tag{22}$$

where N_T is the total hours of the operation and dispatch; N_{DC} is the distributed power sources number; $P_{Gi,t}$ indicates the electrical power of the *ith* distributed power source during the time *t*; $C_f(\cdot)$ indicates the fuel expense of operating the distributed power source; $C_{OM}(\cdot)$ is the expense of maintenance of the distributed power source; N_B indicates the number of make-up boilers; c_{gas} indicates the natural gas price; $H_{Bj,t}$ indicates the thermal power of the *j*th make-up boiler during the time *t*; η_{Bj} is the efficiency of the *j*th make-up boiler; N_x is the number of absorption chillers; $S_{xj,t}$ indicates the cooling power of the *j*th chiller; η_{xj} is denoted as the cooling efficiency; $P_{g,t}$ indicates the power exchanged between the HRS and the main grid during the time *t*; an over 0 value indicates that the HRS sells electricity to the grid, a negative value indicates purchasing electricity from the grid to the HRS; $P_{load,t}$ indicates the power required by the load during the time *t*; $P_{G,t}$ is denoted as the output power of the distributed power supply; $P_{EV,t}$ refers to the charging power of EV; $C_{pp}(\cdot)$ indicates the expense of the purchasing power from the grid; $I_{sp}(\cdot)$ is denoted as the electricity power revenue of the sale from the station to the grid; and f_{C} refers to the cost of participating in carbon transaction.

This multiobjective optimization objective function is:

$$\min F = \lambda_1 \frac{F_1}{F_{1\max}} + \lambda_2 \frac{F_2}{F_{2\max}} \tag{23}$$

The function satisfies $\lambda_1 + \lambda_2 = 1$; in this paper, we take $\lambda_1 = \lambda_2 = 0.5$.

B. Modeling of the Grid Interactions

In this paper, the HRS system adopts the grid-connected operation mode, which indicates that the HRS electrical energy management system can interact with the main grid in both directions: when the energy generated is greater than the system electricity demand, the extra electricity generated can be marketed for economic benefit; when the energy generated by the system is less than the system electricity demand, it can be satisfied by buying electricity from the grid. The mathematical expression is shown below:

$$P_{grid,t} = \begin{cases} P_{grid\text{-}buy,t} = P_{req,t} - \sum_{i=1}^{n} P_{i,t}, & P_{req,t} \geq \sum_{i=1}^{n} P_{i,t} \\ P_{grid\text{-}sell,t} = \sum_{i=1}^{n} P_{i,t} - P_{req,t}, & P_{req,t} < \sum_{i=1}^{n} P_{i,t} \end{cases} \tag{24}$$

$$C_{grid,t} = P_{grid\text{-}buy,t} C_{grid\text{-}buy,t} - P_{grid\text{-}sell,t} C_{grid\text{-}sell,t}$$

where $P_{grid,t}$ denotes the power interaction between the HRS and the grid during time *t*; $P_{grid\text{-}buy,t}$ and $P_{grid\text{-}sell,t}$ are denoted as purchased power and sold power, respectively; $P_{req,t}$ denotes the system electricity demand; $P_{i,t}$ denotes the power output of category *i* generating units during time *t;n* denotes the total number of generating unit types; $C_{grid,t}$ denotes the system interaction cost during time *t*, where a value greater than 0 denotes the purchased power cost and less than 0 denotes that the sold power cost is included in the negative feedback of the integrated operating cost; and $C_{grid\text{-}buy,t}$ and $C_{grid\text{-}sell,t}$ denote the purchased and sold power prices.

C. Constraints

The supply and demand energy balance constraint, along with the controllable unit and storage device output constraint, and the interactive power constraint between the system and the superior grid, are part of the day-ahead economic schedule model of the IES in an HRS. This constraint model has been extensively studied in the literature and will not be repeated in this paper, as the specific formulae can be found in the literature [3].

V. Case Study

A. Basic Data

To demonstrate the rationality of the algorithm model proposed in this paper, a simulation analysis was performed using a typical IES of electricity, thermal and cooling in an HRS as an example. The CCHP unit capacity is 2500 kW, and the electric chiller capacity is 4500 kW. The operating parameters of each unit in this IES are shown in Tables II and III. The natural gas calorific value GHV is 35.54 MJ/m^3, so the price of natural gas purchased from external sources is converted to 0.35 yuan/kWh. Moreover, to facilitate analysis, the natural gas calorific value is 9.7 kWh/m^3, and the unit of natural gas is expressed in kW. In addition, the transferable load is set to 20% of the total load, taking into account the comfort level. The predicted PV output curve and the predicted electric, thermal and cooling load curve for a typical summer day at a selected HRS are shown below [22]. The HRS is equipped with 800 charging piles, of which 400 participate in V2B dispatch. The load dynamic fluctuation curve for air conditioning at an outdoor temperature of 35°C with comfort constraints is shown in Fig. 5.

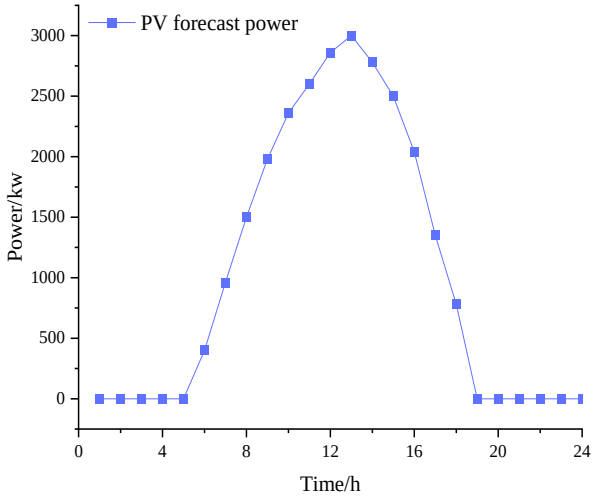

Fig. 3. Typical daily PV output forecast curve for the HRS.

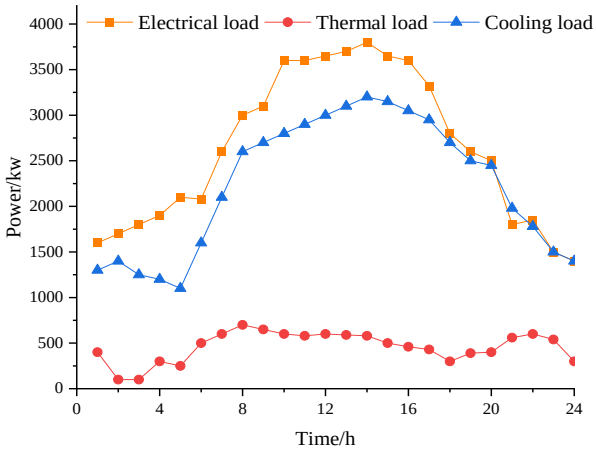

Fig. 4. Typical daily electrical, thermal and cooling load forecast curves for the HRS.

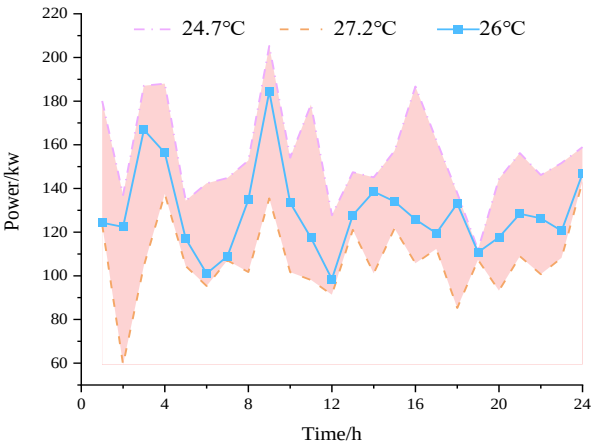

Fig. 5. Dynamic fluctuation curves of air conditioning loads in the HRS under the influence of comfort.

The specifications of each device are shown in Tables II and III.

TABLE II
EQUIPMENT PARAMETERS

Type of equipment	Minimum output(kW)	Maximum output(kW)	Efficiency	Maintenance expense (yuan/kW·h)
CCHP	0	2500	0.45	0.15
GB	200	3800	0.85	0.18
EB	100	1000	0.95	0.10
EC	10	4500	0.95	0.10

TABLE III
ENERGY STORAGE EQUIPMENT PARAMETERS

Type of equipment	Maximum power for charging (kW)	Maximum power for discharging (kW)	Self-consumption rate of equipment	Maintenance expense (yuan/kW·h)
EV	250	300	0.01	-
ES	300	350	0.01	0.018

The DR tariff for the area where the system is located and the grid-distributed generation feed-in tariff, i.e., the time-of-use tariff, are shown in Tables IV and V.

TABLE IV
COMPENSATION PRICES FOR THE DEMAND RESPONSE LOADS

Type of load	Price(yuan/kWh)
Transferable electrical loads	0.16
Reduced electrical load	0.14
Substitutable electrical load	0.12
Transferable thermal load	0.16
Reduced thermal load	0.14
Transferable cold load	0.16
Reduced cold load	0.14

TABLE V
TIME SHARE TARIFF FOR PURCHASE AND SALE OF ELECTRICITY

Time period	Electricity purchase price (yuan/kWh)	Electricity sales price (yuan/kWh)
Peak hours	0.95	0.80
Normal hours	0.65	0.55
Valley hours	0.38	0.35

B. *Results Analysis*

To demonstrate the correctness of the integrated energy optimization control algorithm advanced in this paper, the following three scenarios are established to compare and analyze the system performance in different scenarios, as shown in Table VI, of which Scenario 3 is the proposed optimization control model in this paper.

TABLE VI
SCENARIO COMPARISON TABLE

Scenario Type	carbon trading constraints	electrical load interaction	hot and cold load interaction
Scenario 1	√	×	×
Scenario 2	√	√	×
Scenario 3	√	√	√

Carbon allowances are calculated using a fixed value, with a base carbon emission overrun penalty fee of 0.50 yuan/kg, an interval length of 500 kg of carbon emissions, and a penalty price increase of 25%.

Optimization results

The optimization results of Scenario 3 are analyzed. Fig. 6 shows the curve for the optimal arrangement of the electric output of each piece of equipment in this scenario, Fig. 7 indicates the curve for the optimal arrangement of the heating of each piece of equipment, and Fig. 8 indicates the curve for the optimal arrangement of the cooling of each piece of equipment. On the prerequisite of satisfying the three load demands of electricity, thermal and cooling in the HRS, the optimal arrangement of the IES in the HRS participating in the carbon transaction market under the DR is considered so that the supply, storage and energy-use systems are dynamically balanced to achieve efficient and economic operation in the HRS.

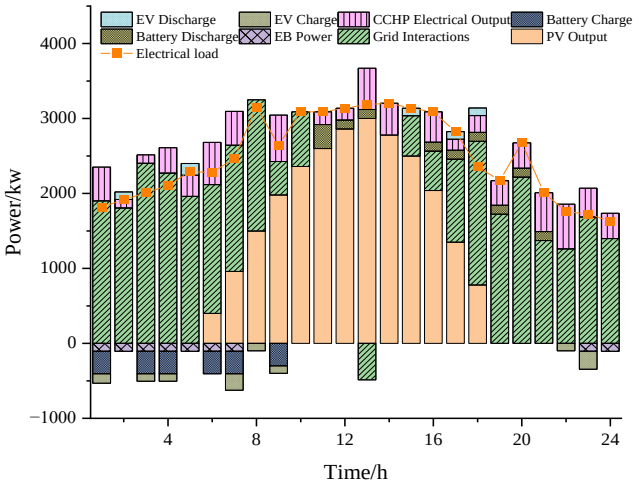

Fig. 6. Power output under electrical balance.

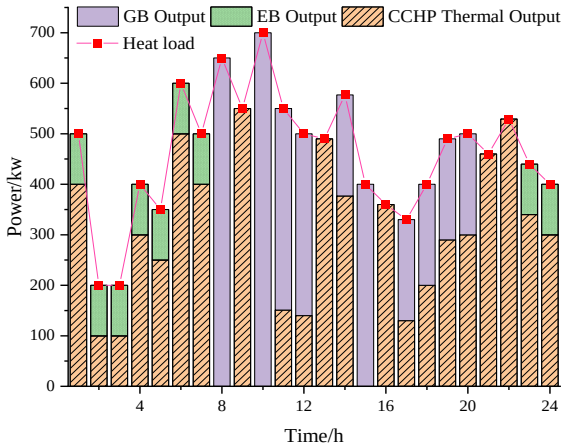

Fig. 7. Thermal output under thermal balance.

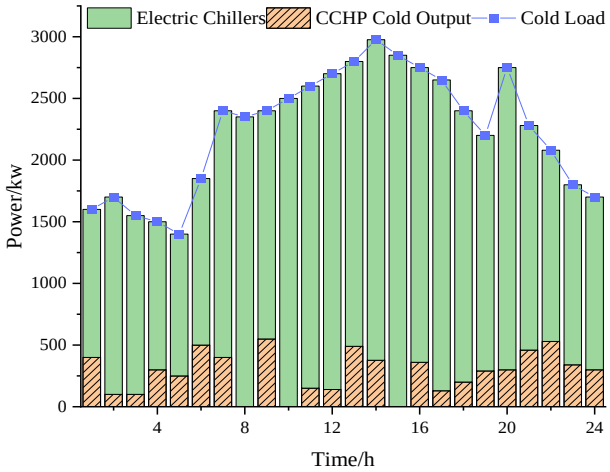

Fig. 8. Cold output under cold balance.

As shown in Fig. 6 to Fig. 8, the system will arrange the output according to the grid tariff as the grid implements peak and valley tariffs. During the peak phase of the tariff, the CCHPs are called upon to provide the cooling and thermal sources in priority, while the distributed PV and CCHPs are called upon to supply power, with the shortfall being supplemented by the grid. The CCHPs operate in a more flexible manner, with the system in a state of active response and interaction with the grid.

The charging process of the EVs involved in V2B dispatch is shown in Fig. 9; the working state of the battery is shown in Fig. 10. Moreover, 1:00-7:00 is the low power consumption period, and the electric vehicle group and the battery are actively dispatched to charge and store energy to fill the low power consumption. In addition, 11:00-21:00 is the peak power consumption period, and the electric vehicle group and the battery are dispatched to discharge to replenish the power used by the CCHP station and reduce the peak. The V2B dispatching of electric vehicles and storage batteries cooperates with each other, and comprehensive dispatching has reduced the fluctuation of electricity consumption in the grid and stabilized the use of electricity in the HRS.

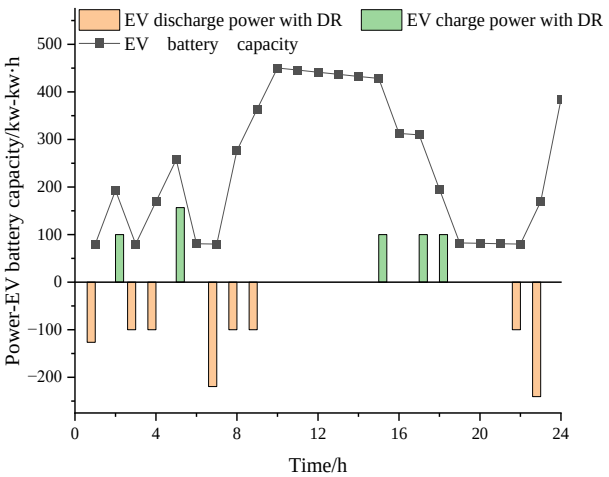

Fig. 9. Charging and discharging of electric vehicles involved in V2B dispatch.

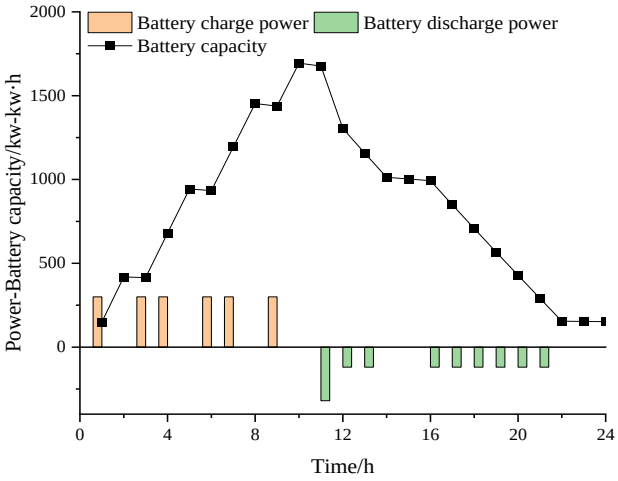

Fig. 10. Working condition of energy storage batteries.

As seen in Fig. 9 to Fig. 10, the system schedules the charging process of EVs and batteries according to the current power consumption of the grid, as there is a peak-to-valley gap in the grid. In the peak phase of electricity consumption, the battery and V2B dispatching EV group are called in priority to supply electricity. In the low phase of electricity consumption, the V2B dispatches the electric vehicle fleet to charge first and arranges for the battery to charge and standby, with the two operating in interaction with the grid to achieve efficient use of energy.

Scenario comparison

Regarding the comparison of scenarios, the findings are summarized in Table VII. It can be observed that when the IES of the HRS is involved in carbon transactions, the advantages of new energy generation can be fully utilized to obtain the benefits of cost reduction, verifying that the optimized operation method proposed in this paper, which considers the coupling of carbon market trading and participation in the demand response mechanism, improves the system operation cost, in which scenario 3 reduces the operation cost by 18.81% and 9.62% compared with scenarios 1 and 2, respectively.

TABLE VII
COST COMPARISON IN THREE SCENARIOS

	Scenario 1	Scenario 2	Scenario 3
Energy costs/yuan	11582	12965	11207
Grid interaction costs/yuan	24839	26153	18494
Operation and maintenance costs/yuan	7755.6	3444.1	9019.4
Demand response compensation/yuan	0	1090.7	1454.9
Carbon market revenues/yuan	5981.1	7163.4	6256.4
Total costs/yuan	38195	34308	31009

The effect of the DR on the charging and discharging of the EV fleet in the IES of the HRS is shown in Fig. 11. When the DR of the electrical load is not considered, the electric vehicle fleet cannot make full use of its charging and discharging advantages and actively interact with the grid, so the effect of smoothing out grid fluctuations cannot be achieved.

Fig. 12 to Fig. 14 show the influence of the DR on the electrical, thermal and cold loads within the IES of the HRS.

As shown in Fig. 12 to Fig. 14, the comfortable level DR mechanism is used to adjust load fluctuations within the comfortable level range, as shown in Fig. 5. To ensure the comfortable level of the users in the HRS, the optimized load shows a trend of peak shaving and valley filling due to the high reliability requirements for the supply of cold energy. Therefore, the IES of the HRS participates in the grid DR, and on the premise of satisfying the comfort level of the users regarding the electricity, thermal and cold, the

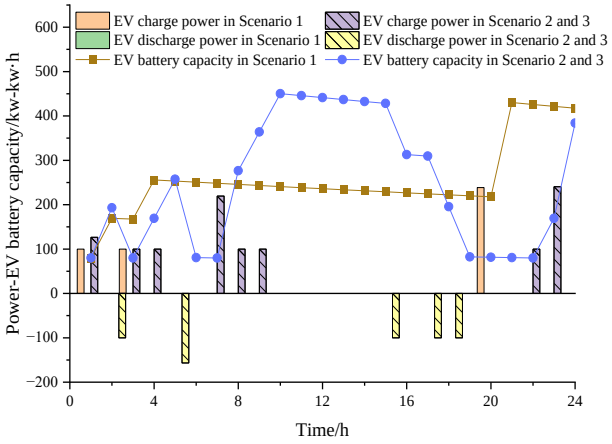

Fig. 11. Scenario comparison of electric vehicle charging and discharging.

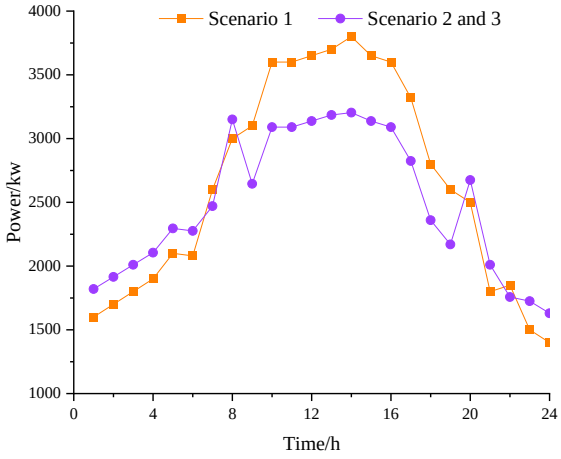

Fig. 12. Scenario comparison of electrical loads.

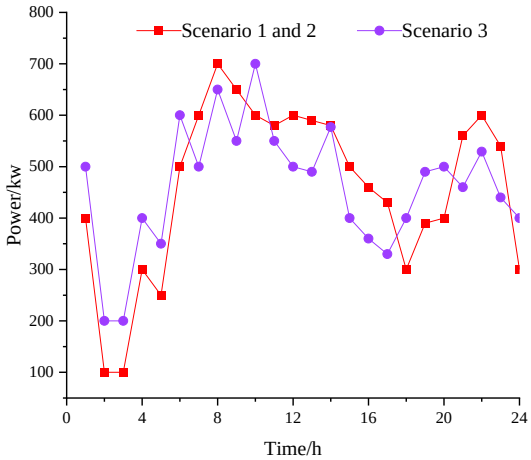

Fig. 13. Scenario comparison of the thermal loads.

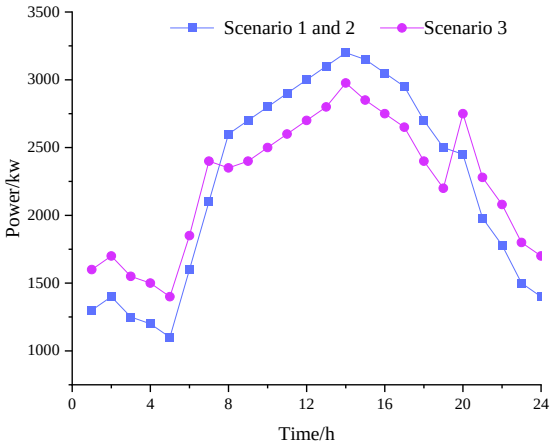

Fig. 14. Scenario comparison of cold loads.

system actively participates in the grid interaction upward to arrange the power output of the electric thermal and cooling equipment and actively participates in carbon transaction downward to low carbon operations and cost reductions.

Sensitivity analysis

By analyzing the effect of different trading base prices λ on E_{PIES} under scenario 3, the effect of the optimized operation method of participating in the carbon trading mechanism proposed in this paper on the improvement of system operation cost is verified. The results are shown in Fig. 15. When the trading base price λ is increased from 0.25 to 0.5, 1, 2, 3, 4 and 5 in order, compared with the base price of 0.5 set in this paper, the actual carbon savings E_{PIES} within the IES in the HRS are increased by -2.66%, 2.84%, 3.91%, 4.98%, 5.33% and 5.33%, respectively.

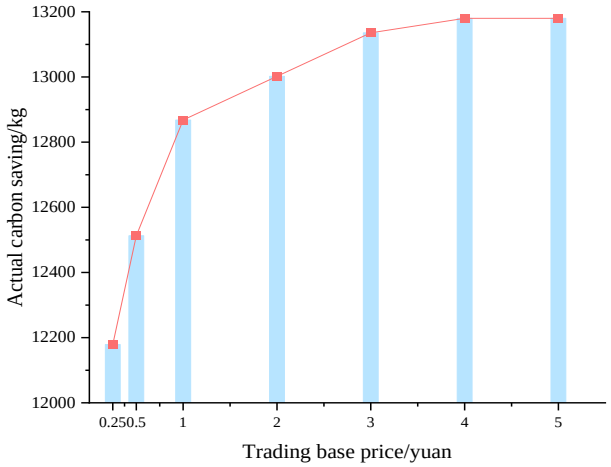

Fig. 15. Sensitivity analysis of trading base price.

As shown in the results of Fig. 15, it can be concluded that when the HRS participates in the carbon trading market, the increase in the trading base price in the carbon trading market has a certain positive promotion and positive guiding effect on the energy saving and emission reduction operation of the integrated energy system in the HRS, but due to the limited resources in the station and the consideration of the users' energy comfort constraint, it leads to a certain limitation of this carbon reduction effect, and when the energy in the station has been fully dispatched, even if the trading base price continues to increase, the energy saving promotion effect cannot be achieved.

VI. Conclusion

This paper presents an allocation strategy for the IES of an HRS, taking into account the combined effects of participation in the carbon transaction market and meeting the comfort level of the user side. Based on the reality of coupling new energy outputs and multiple loads of cooling, heating and electricity in the HRS, our goal is to boost the energy efficiency in the station and stabilize the balance of supply and demand in the station by taking advantage of the transferable characteristics of energy storage and the additional revenue brought by the carbon transaction market to effectively improve the revenue of the HRS and fully exploit the DR potential of the integrated energy in the station while maintaining the stability of the station and realizing the economic performance and low-carbon operation in the stations. Through multiple situations comparative analysis, the practicality and usefulness of the method advanced in this paper has been fully proven. Successfully achieving the carbon emission intensity target under the premise of ensuring sustainable economic development is crucial to the long-term development of each country. Therefore, an optimal DR dispatching strategy that couples the consideration of participation in the carbon transaction market and satisfaction of user-side comfort in the HRS scenario will become an optimal dispatching strategy worth promoting for application. It provides a good promotion effect for the implementation of various scheduling strategies in other scenarios, lays the foundation for the carbon market to give full play to the role of the green economy in future power consumption scenarios, and provides more optimization angles for energy-saving optimization on the customer's building side.

References

[1] Xiaodan Yu, Xiaodong Xu, Shuoyi Chen, Jianzhong Wu, and Hongjie Jia, "A brief review to integrated energy system and energy internet," *Diangong Jishu Xuebao/Transactions of China Electrotechnical Society*, vol.31, no.1, pp1-13, 2016.

[2] Kecheng Li, Huaguang Yan, Guixiong He, Chengzhi Zhu, Kaicheng Liu, and Yuting Liu, "Seasonal Operation Strategy Optimization for Integrated Energy Systems with Considering System Cooling Loads Independently," *Processes*, vol.6, no.10, pp202, 2018.

[3] Lixia Cao, Yujing Huang, and Nian Liu, "Optimal Scheduling of Building Integrated Energy System considering uncertainty of Human Behavior," *2021 3rd International Academic Exchange Conference on Science and Technology Innovation (IAECST)*. IEEE, 2021.

[4] Omine, Eitaro, Hiroyuki Hatta, and Tsuyoshi Ueno, "A study of economic feasibility of Smart Community-calculation of profit of Community Operator considering introduction of battery and co-generation systems," *2016 IEEE Power & Energy Society Innovative Smart Grid Technologies Conference (ISGT)*. IEEE, 2016.

[5] Yamagata, Yoshiki, Hajime Seya, and Sho Kuroda, "Energy resilient smart community: Sharing green electricity using V2C technology," *Energy Procedia*, vol.61, pp84-87, 2014.

[6] Ollivier, Gerald, Richard Bullock, Ying Jin, and Nanyan Zhou, "High-speed railways in China," 2014.

[7] Dawei Wu, and Ruzhu Wang, "Combined cooling, heating and power: A review," *progress in energy and combustion science*, vol.32, no.5-6, pp459-495, 2006.

[8] Shaochao Ma, and Ying Fan, "A deployment model of EV charging piles and its impact on EV promotion," *Energy Policy*, vol.146, pp111777, 2020.

[9] Li Yang, Meng Han, Zhen Yang, and Guoqing Li, "Coordinating flexible demand response and renewable uncertainties for scheduling of community integrated energy systems with an electric vehicle charging station: A bi-level approach," *IEEE Transactions on Sustainable Energy*, vol.12, no.4, pp2321-2331, 2021.

[10] Lei Huang, Xiaoyan Zhang, Xi Ding, and Chuangxin Guo, "Analysis of Commercial Model of Park-level Integrated Energy System Participating in Carbon Trading Considering Electric Vehicles," *2021 International Conference on Power System Technology (POWERCON)*. IEEE, 2021.
[11] Parvania, Masood, and Mahmud Fotuhi-Firuzabad, "Demand response scheduling by stochastic SCUC," *IEEE Transactions on smart grid*, vol.1, no.1, pp89-98, 2010.
[12] D'Arco, Salvatore, Luigi Piegari, and Pietro Tricoli, "Comparative analysis of topologies to integrate photovoltaic sources in the feeder stations of AC railways," *IEEE transactions on transportation electrification*, vol.4, no.4, pp951-960, 2018.
[13] Qingbo Cheng, "Energy management system of a smart railway station considering stochastic behaviour of ESS and PV generation," *2018 International Symposium on Computer, Consumer and Control (IS3C)*. IEEE, 2018.
[14] Perez Filipe, Iovine Alessio, Damm Gilney, Galai-Dol Lilia, and F. Ribeiro Paulo, "Stability analysis of a DC microgrid for a smart railway station integrating renewable sources," *IEEE Transactions on Control Systems Technology*, vol.28, no.5, pp1802-1816, 2019.
[15] Hayashiya Hitoshi, Itagaki Hiroshi, Morita Yuichi, Mitoma Yoshihisa, Furukawa Takayuki, Kuraoka Takuya, Fukasawa Yuta, and Oikawa Takatoshi, "Potentials, peculiarities and prospects of solar power generation on the railway premises," *2012 International Conference on Renewable Energy Research and Applications (ICRERA)*. IEEE, 2012.
[16] Pankovits, P., Pouget J., Robyns B., Delhaye F., and Brisset S., "Towards railway-smartgrid: Energy management optimization for hybrid railway power substations," *IEEE PES Innovative Smart Grid Technologies, Europe*. IEEE, 2014.
[17] Boudoudouh, Soukaina, and Mohammed Maaroufi, "Renewable energy sources integration and control in railway microgrid," *IEEE Transactions on Industry Applications*, vol.55, no.2, pp2045-2052, 2018.
[18] Svendsen, Harald G., Ahmed A. Shetaya, and Khalid Loudiyi, "Integration of renewable energy and the benefit of storage from a grid and market perspective-results from Morocco and Egypt case studies," *2016 International Renewable and Sustainable Energy Conference (IRSEC)*. IEEE, 2016.
[19] Spash, Clive L, "The brave new world of carbon trading," *New Political Economy*, vol.15, no.2, pp169-195, 2010.
[20] Pazhoohesh, Mehdi, and Cheng Zhang, "A satisfaction-range approach for achieving thermal comfort level in a shared office," *Building and Environment*,vol.142, pp312-326, 2018.
[21] Xinyu Tian, Huake Su, Fan Wang, Kun Zhang, and Qinghe Zheng, "A Electric Vehicle Charging Station Optimization Model Based on Fully Electrified Forecasting Method," *Engineering Letters*, vol. 27, no.4, pp731-743, 2019.
[22] Xuan Xuan, Yan Zhao, Yucai Li, Ruyu Zhang, and Ping Zhang, "Research on Short-term Load Forecasting Model of Integral Energy System Considering Demand Side Response," *IAENG International Journal of Computer Science*, vol. 47, no.3, pp599-604, 2020
[23] Junsheng Huang, Huanping Huang, Xiaoping Guang, Rong Li, and Jianshu Zhu, "Bi-level Programming Model to Solve Facility Configuration and Layout Problems in Railway Stations," *Engineering Letters*, vol. 26, no.3, pp364-371, 2018